Recombination of bare Bi^{83+} ions with electrons

A. Hoffknecht, C. Brandau, T. Bartsch, C. Böhme, H. Knopp, S. Schippers, and A. Müller
Institut für Kernphysik, Universität Giessen, D-35392 Giessen, Germany

C. Kozhuharov, K. Beckert, F. Bosch, B. Franzke, A. Krämer, P. H. Mokler, F. Nolden, M. Steck, and Th. Stöhlker
Gesellschaft für Schwerionenforschung (GSI), D-64291 Darmstadt, Germany

Z. Stachura
Institute for Nuclear Physics, 31-342 Kraków, Poland

(Received 15 March 2000; revised manuscript received 8 August 2000; published 5 December 2000)

Electron-ion recombination of completely stripped Bi^{83+} has been investigated at the Experimental Storage Ring (ESR) of the GSI in Darmstadt. Absolute recombination-rate coefficients have been measured for relative energies between ions and electrons from 0 up to about 125 eV. In the energy range from 15 meV to 125 eV, the experimental result is well described by the theory for radiative recombination (RR). However, below 15 meV the experimental rate increasingly exceeds the RR calculation by up to a factor of 5.2. This puzzling enhancement phenomenon, which has already been observed at other storage rings and single-pass merged-beams setups, is reported here from the ESR and for a bare ion heavier than argon. The enhancement is insensitive to changes of the electron density, which in subsequent measurements was set to 1.6×10^6, 3.2×10^6, and $4.7\times10^6\ cm^{-3}$. An additional variation of the magnetic guiding field of the electrons from 70 mT to 150 mT in steps of 1 mT resulted in oscillations with a period of 7.6 mT of the rate that are accompanied by considerable changes of the transverse electron temperature.

DOI: 10.1103/PhysRevA.63.012702 PACS number(s): 34.80.Lx, 29.20.Dh

I. INTRODUCTION

Recombination between electrons and highly charged ions plays an important role in different areas of modern physics. The basic two- and three-body recombination processes are of very fundamental nature and thus provide an excellent testing ground for collision theory and atomic structure calculations. Cross sections and rate coefficients as a function of the relative energy of these processes are needed for the understanding of astrophysical and fusion plasmas. Additionally, they provide useful information for applications in accelerator physics [1], since beam losses in ion storage rings by electron-ion recombination during electron cooling post harsh limits to the handling and the availability of ions for further experiments.

Low-energy electron-ion recombination with its large cross sections and rates provides a very promising scheme for the production of antihydrogen by recombination of cold positrons with antiprotons [2]. At very low temperatures and in the presence of magnetic fields of the ion traps, the expected recombination rates are uncertain by an order of magnitude. Recombination rates as enhanced as those observed in storage rings and single-pass merged-beams experiments would facilitate the production of antihydrogen in quantities needed for the envisaged spectroscopy experiments. The question to what extent electromagnetic fields can enlarge recombination rates especially at the low temperatures envisaged for antihydrogen production is currently pursued [3]. In this context, storage-ring electron coolers provide an excellent environment for a further exploration of low-energy electron-ion recombination in the presence of external magnetic fields.

During the past decade, electron-ion recombination has been extensively investigated in merged-beam experiments using storage-ring coolers and single-pass electron targets at accelerators. In these experiments, an incident ion beam is merged with a cold magnetically guided beam of electrons over a distance of typically 50–250 cm depending on the specific electron-beam device. By choosing the appropriate accelerator facility, ions of most elements in all possible charge states can be investigated nowadays.

Free electrons can be captured by ions via several different mechanisms. The main recombination channel for a bare ion is radiative recombination (RR),

$$e^- + A^{q+} \rightarrow A^{(q-1)+} + h\nu. \tag{1}$$

RR is the direct capture of a free electron by an ion A^{q+} where the excess energy and momentum are carried away by a photon. After the capture, which is inverse to photoionization, the electron can be in an excited state and there will be further radiative transitions within the ion until the electron has reached the lowest accessible energy level. RR is a nonresonant process with a diverging cross section at zero center-of-mass (c.m.) energy that continuously decreases towards higher c.m. energies.

Another recombination mechanism possible for a bare ion is three-body recombination (TBR),

$$A^{q+} + e^- + e^- \rightarrow A^{(q-1)+} + e', \tag{2}$$

where the excess energy and momentum are carried away by a second electron. This process is important at high electron densities and low c.m. energies between electrons and ions.

The pioneering experiment on radiative recombination of bare ions was performed by Andersen *et al.* [4] in 1990. Absolute rate coefficients were measured for C^{6+} with a merged-beam technique finding a reasonably good agree-

ment between experiment and theory in the investigated energy range from $E_{rel}=0$ to 1 eV, where E_{rel} is the relative energy between the ensembles of electrons and ions in the interaction region (for the definition of E_{rel}, see Sec. III).

In a number of consecutive measurements, different bare ions (D^+,He^{2+},C^{6+},N^{7+},Ne^{10+},Si^{14+},Ar^{18+}) [5–8] have been investigated at several facilities. The measured rate coefficients have been in accordance with RR theory for relative energies $E_{rel}\geqslant 0.01$ eV. Except for a dedicated study with Cl^{17+} ions [9], the experiments were limited by counting statistics to an energy range of only a few eV. Nevertheless, in all of these measurements, strong deviations of the experimental findings from the theoretical predictions were found at very low electron-ion relative energies ($E_{rel}\leqslant 0.01$ meV). Toward lower energies, the measured rate coefficient α_{exp} [the velocity averaged product of velocity and cross section, see Eq. (12)] typically shows an increase $\Delta\alpha=\alpha_{exp}-\alpha_{RR}$ on top of the theoretical rate coefficient α_{RR} for RR. The resulting rate enhancement factor $\epsilon=\alpha_{exp}/\alpha_{RR}$ at $E_{rel}=0$ eV was observed to take values of 1.6 (He^{2+}) to 10 (Ar^{18+}) for bare ions (no enhancement observed with D^+) and up to 365 for a multicharged multielectron system such as Au^{25+} [10]. It should be noted that in contrast to the RR cross section that diverges at $E_{rel}=0$ eV, the measured rate coefficient attains a finite value due to the experimental electron and ion velocity spreads (see Sec. III).

Since the first observation of the enhancement phenomenon in an experiment with U^{28+} ions at the GSI in Darmstadt in 1989 [11] and a later experimental confirmation of that same result [12], this effect has been observed repeatedly in different experiments at different facilities. Whereas the very high rate enhancement factors of multicharged complex ions such as Au^{25+}, Au^{50+}, Pb^{53+}, and U^{28+} could be partly traced back to the presence of additional recombination channels, i.e., mainly due to dielectronic recombination (DR) [10,13–15], the origin of the remaining discrepancies between experiment and theory especially for bare ions, where DR cannot occur, is still unknown. Among the mechanisms that have been further discussed are polarization recombination [16], TBR [17], and a momentum coherence effect in time-varying fields [18]. Also, plasma-physical aspects such as the transient behavior of the nonequilibrium plasma formed by merged beams [19] and the screening dynamics of the magnetized electron gas in an electron cooler [20,21] have been explored. However, none of these efforts has been successful in explaining the enhancement phenomenon so far.

For the further experimental exploration of the enhancement phenomenon, its dependences on external experimental parameters have been studied at different storage rings. Variations of the electron density [8,9,22] within a total range from about $10^6\,cm^{-3}$ up to almost $10^{10}\,cm^{-3}$ showed almost no effect on the enhancement. The dependence of the total recombination rate followed the $T_\perp^{-1/2}$ dependence on the mean transverse electron energy spread $T_\perp$ [22] as expected for RR alone. Moreover, Gwinner *et al.* [22] discovered an extra $T_\parallel^{-1/2}$ scaling of the excess rate $\Delta\alpha$, which is not expected [23] on the basis of the sheer convolution of any given $1/E^x$-dependent cross section ($x>0$) with the experimental velocity distribution describing merged-beam kinematics [see Eq. (13)]. A systematic study of the ion charge-state dependence of the excess rate coefficient $\Delta\alpha$ for a number of bare ions [5] yielded roughly a $Z^{2.8}$ scaling for atomic numbers $1\leqslant Z\leqslant 14$. Another external parameter observed to influence the enhancement has been the magnetic-field strength B in the interaction region of electrons and ions. A clear increase of the recombination-rate maximum at $E_{rel}=0$ with increasing magnetic-field strength has been found in an experiment using Au^{25+} ions [10]. Recently, such a behavior has also been observed in a thorough study with lithiumlike F^{6+} and bare C^{6+} ions at the TSR heavy-ion storage ring in Heidelberg [22,24]. In these experiments, an approximate B^x scaling ($0.5\leqslant x\leqslant 1$) of $\Delta\alpha$ has been found.

At the present stage of the game where numerous theoretical approaches and model treatments of the enhancement phenomenon have failed to provide a consistent picture, it appears necessary to provide experimental information on the dependence of the rate enhancement on the widest possible range of parameters such as to narrow down the range of possible explanations and to search for hints to the origin of a disturbing experimental observation that has puzzled experimentalists and theorists for a decade already. Understanding this phenomenon will not only help in avoiding intensity losses of stored ions during cooling and taking advantage of enhanced rates for antihydrogen production, it will most likely shed new light on the understanding of electron-ion cooling. Last but not least, the observed dilemma of a very fundamental atomic collision process at very low energies certainly has to be resolved.

In the present measurement with Bi^{83+} ions, which was carried out at the Experimental Storage Ring of the GSI in Darmstadt, we extended the investigations of bare ions to the range of highest possible charge states. To our knowledge, it was the first experiment of this kind with such a bare ion heavier than argon providing information on RR at low energies. It should be noted that at higher electron-ion c.m. energies, experimental information about RR cross sections has already been obtained from studies of radiative electron capture (REC) in high-energy ion-atom collisions [25,26]. Here we present a comparison of measured absolute rate coefficients with calculated RR rates for relative energies from $E_{rel}=0$ eV to 125 eV. This constitutes a test of the validity of the most advanced theoretical approaches to recombination in the regime where relativistic and QED effects are important. In addition, the dependence of the recombination rate on the electron density of the electron beam in the cooler was investigated in order to study the enhancement phenomenon and to check whether our experimental approach yields consistent results under different experimental conditions. The present paper is organized as follows. After a short description of the theoretical approaches, the experimental setup is described with a focus on the details of the merged beam arrangement inside the ESR electron cooler. After the presentation of the experimental results, a comparison with RR calculations is made that features the rate enhancement phenomenon at very low energies. Dependences of the mea-

sured rate at zero relative energy on beam alignment, electron density, and magnetic guiding field are explored and discussed in detail.

II. THEORY

In order to describe RR theoretically, Kramers developed a semiclassical theory already in 1923 [27]. A full quantum-mechanical treatment within the nonrelativistic dipole approximation was performed by Stobbe seven years later [28]. In 1957, Bethe and Salpeter [29] derived an approximate semiclassical formula for the RR cross section that is identical to Kramers' result,

$$\sigma_{\mathrm{RR}}(n,E_{\mathrm{cm}})=\sigma_0\frac{E_0^2}{nE_{\mathrm{cm}}(E_0+n^2E_{\mathrm{cm}})} \tag{3}$$

with $\sigma_0\approx 2.1\times 10^{-22}\,\mathrm{cm}^2$. The capture of an electron by a bare ion produces a hydrogenic state with principal quantum number n. In this case, $E_0=Z^2\mathcal{R}$ is the binding energy of the ground-state electron in the hydrogenic ion (atom) with nuclear charge Z, $\mathcal{R}\approx 13.6$ eV is the ground-state energy of the hydrogen atom, and E_{cm} is the kinetic energy in the electron-ion c.m. frame. The total cross section for this process is obtained by summing up the contributions of all accessible Rydberg states:

$$\sigma_{\mathrm{RR}}(E_{\mathrm{cm}})=\sum_{n=1}^{n_{\max}}\sigma_{\mathrm{RR}}(n,E_{\mathrm{cm}}), \tag{4}$$

where $n_{\max}$ is the maximum principal quantum number that can contribute. This number is generally limited by experimental conditions. Since the contributions by high-n states to the total RR cross sections become smaller with increasing n, a very precise knowledge of $n_{\max}$ is not required for a meaningful comparison of experiment with RR theory. The approach of Bethe and Salpeter clearly shows the typical features of RR cross sections: the divergence at zero electron energy and a monotonic decrease for increasing electron energy. However, as a semiclassical approximation, Eq. (3) is only valid in the limit of high quantum numbers and low electron energies, i.e., for $n\gg 1$ and $E_{\mathrm{cm}}\ll\mathcal{R}(Z/n)^2$. Since the quantum-mechanical treatment of Stobbe involves the rather tedious evaluation of hydrogenic dipole matrix elements, one often applies correction factors $G_n(E_{\mathrm{cm}})$, the so-called Gaunt factors, to Eq. (3) to account for deviations from the correct quantum result at low n and high E_{cm}. The use of Gaunt factors is convenient because they are either tabulated [30] or given in an easy parametrization [31,32]. We apply here tabulated [33] values $k_n=G_n(0)$ and use

$$\sigma_{\mathrm{RR}}(E_{\mathrm{cm}})=\sigma_0\sum_{n=1}^{n_{\max}}k_n\frac{(Z^2\mathcal{R})^2}{nE_{\mathrm{cm}}(Z^2\mathcal{R}+n^2E_{\mathrm{cm}})}. \tag{5}$$

This equation is exact for bare ions at zero relative energy and does not deviate by more than about 0.8% for $Z=83$ and $n_{\max}=116$ from the quantum mechanically correct result within the nonrelativistic dipole approximation at the highest energies considered in this paper. In contrast, the approach

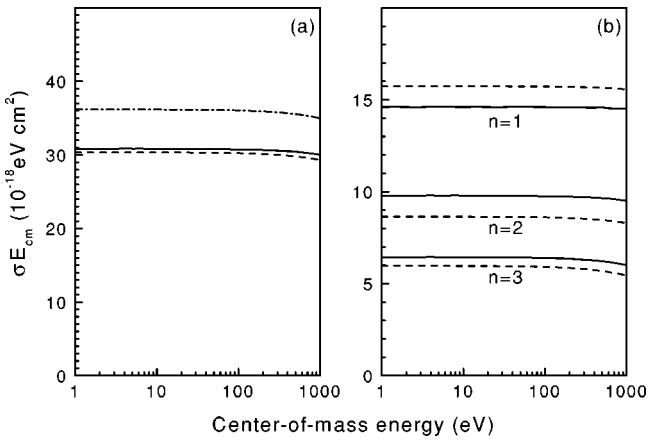

FIG. 1. Theoretical cross sections for radiative recombination of bare Bi^{83+} ions as a function of c.m. energy. (a) Comparison between n-summed ($n_{\max}=3$) fully relativistic [34] (full line), semiclassical Gaunt-factor-corrected [cf. Eq. (5)] (dashed line) and -uncorrected [cf. Eq. (4)] (dash-dotted line) calculations. In order to remove the divergence at $E_{\mathrm{cm}}=0$, the cross sections have been multiplied by E_{cm}. (b) n-selective comparison between fully relativistic (full lines) and Gaunt-factor-corrected semiclassical [cf. Eq. (5)] (dashed lines) calculations for $n=1,2,3$. Differences between results of Eq. (5) and the quantum mechanically exact nonrelativistic dipole approximation are not visible in the energy range of the figure.

without Gaunt factors used by Bethe and Salpeter [cf. Eq. (4)] differs by as much as $\sim 11\%$ [see Fig. 1(a)] from the quantum mechanically correct result.

For heavy ions with high nuclear charge and for high energies, the validity of the nonrelativistic dipole approximation is questionable. This is already evident when one compares the binding energy of the $Bi^{83+}(1s_{1/2})$ ground state calculated with the Rydberg formula [entering Eq. (5)] to $E_0=Z^2\mathcal{R}\approx 93$ keV with the value of $E_0=m_ec^2[1-\sqrt{1-(\alpha Z)^2}]\approx 104.4$ keV from Dirac theory [29] (c denotes the speed of light and $\alpha=1/137.036$). In general, an exact relativistic calculation within the framework of Dirac theory and with the inclusion of higher multipoles is in order. Results of such calculations for bare ions with $1\leqslant Z\leqslant 120$ and $n\leqslant 3$ have recently been presented by Ichihara and Eichler [34]. When comparing their result for Bi^{83+} with the outcome of Eq. (5) with $Z=83$ and $n_{\max}=3$, we find that over the experimental energy range, the maximum difference is only less than 2% [cf. Fig. 1(a)]. This is due to cancellation effects as shown in Fig. 1(b), where the contributions by each individual n are plotted separately. The differences between the relativistic and nonrelativistic calculations change sign when going from $n=1$ to $n=2$. The absolute difference is largest for $n=1$ (up to $\sim 7\%$). In general, relativistic effects become weaker with increasing n. Therefore, we do not expect that the difference increases when extending the summation to higher principal quantum numbers. Since the 2% maximum deviation of the n-summed nonrelativistic dipole approximation from the fully relativistic calculation is smaller than the experimental uncertainty, we use Eq. (5) for all calculations presented in this paper. It is noted that at high c.m. energies (100 keV$\gtrsim E_{\mathrm{cm}}\gtrsim m_ec^2$), a good agreement be-

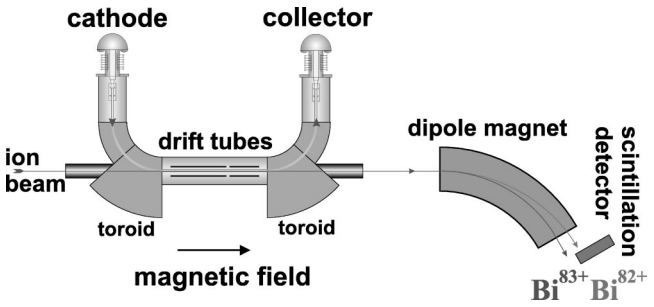

FIG. 2. Schematic view of the ESR electron cooler and the experimental setup for recombination measurements. The cold electron beam produced in the gun is guided by the magnetic field and merged with the ion beam over a distance of 2.5 m. The electron beam is then separated from the ion beam by the magnetic guiding field and transferred to the collector. Recombined and parent ions that leave the cooler together are separated from each other in the first dipole magnet after the cooler. A scintillator detector is used to count the recombined particles.

tween results of the nonrelativistic dipole approximation and experimental REC cross sections has already been found by Stöhlker *et al.* [35]. Finally, we mention that calculations of QED corrections to the RR cross section into the $n=1$ shell have recently been performed by Shabaev *et al.* [36]. They find that QED corrections increase in magnitude with increasing electron energy. Since for bare uranium ions the calculated QED corrections amount to only 0.12% at the lowest c.m. energy of $\sim$54.5 keV considered in Ref. [36], QED corrections can safely be neglected in the present study.

III. EXPERIMENT

The measurements have been performed at the Experimental Storage Ring (ESR) of the Gesellschaft für Schwerionenforschung (GSI) in Darmstadt [37]. 295.3 MeV/u Bi^{83+} ions supplied by the GSI linear accelerator UNILAC in combination with the heavy-ion synchrotron SIS were injected into the ESR. Only one injection pulse of ions from the SIS into the ESR was sufficient to provide an ion current of typically 400–800 μA at the beginning of a measurement. In the storage ring, the circulating Bi^{83+} ions were merged with the magnetically guided electron beam of the electron cooler with an electron energy of 162 keV (Fig. 2). An optimum beam alignment is achieved by using steering coils for centering the electron beam onto the ion beam. The beam alignment can be monitored by observation of the cooling force and the ion-beam profiles. Before starting a measurement, the ion beam was cooled for several seconds until the beam profiles reached their equilibrium widths. For a change of the electron energy, voltages between -5 and 5 kV were applied to two drift tubes surrounding the electron and the ion beam in the interaction region. During a measurement cycle, the electron energy was stepped through a preset range of values different from the cooling energy, thus introducing nonzero mean relative velocities v_{rel} between ions and electrons. In between two measurement steps a cooling interval was inserted such that during one energy scan the drift tube voltages were meandering from the lowest to the highest preset values. The voltages were supplied by a system of 16 individual power supplies controlled by fast high-voltage switches. This instrument has been constructed specially for recombination experiments [38]. Only 2 ms are needed by this device to switch to and set a certain voltage with a relative precision of 10^{-4}. The repetition rate of voltage settings with this precision is limited to 40 per second.

Recombined Bi^{82+} ions were counted as a function of the electron energy on a scintillator detector located behind the first dipole magnet downstream of the electron cooler. The dipole magnet bends the circulating Bi^{83+} ion beam onto a closed orbit and separates the recombined Bi^{82+} ions from that orbit. In between two measurement steps of 40-ms duration each, the electron energy was always set to the cooling energy ($E_{\mathrm{rel}}=0$) for 20 ms in order to maintain good ion-beam quality. The experimental data stream was continuously collected and stored after each ms. The time-resolved measurements allowed us to observe and eliminate drag force effects from the data in a detailed off-line analysis. Such effects are a result of the cooling force exerted by the electrons on the ion beam, which can lead to a time-dependent shift of the ion velocity towards the electron velocity. The friction forces are particularly effective at relative energies close to zero. It is therefore expected that for long times at off-cooling energies, the relative energy between electrons and ions changes to lower values than nominally set. If this were the case, spectra recorded at later time intervals would exhibit features at higher nominal energies compared to spectra taken at earlier time intervals where the same features appear at lower energies. Such shifts have not been observed in our time-dependent data analysis. Therefore, we conclude that drag forces are not effective during the 40-ms measurement time intervals.

The kinetic energy E_e of the electrons is defined by the cathode voltage U_{gun} ($=-162$ kV in this experiment), the drift tube voltage U_{drift}, and the space-charge potential U_{sp} in the interaction region. Assuming coaxial beams, it is calculated as

$$E_e = -eU_{\mathrm{gun}} + eU_{\mathrm{drift}} - eU_{\mathrm{sp}} = -eU_{\mathrm{gun}} + eU_{\mathrm{drift}} - \frac{I_e r_e m_e c^2}{e v_e}[1+2\ln(b/a)], \quad (6)$$

where r_e is the classical electron radius. The quantities $b=10$ cm and $a=2.54$ cm are the radii of the drift tube and the electron beam, respectively. The ion-beam diameter is only of the order of a millimeter and, hence, the electron energy distribution probed by the ions is rather flat across the ion beam. In the present experiment, we performed measurements with different electron currents I_e that produced space-charge potentials ranging from +17.2 V to +51.7 V.

The space-charge corrected electron energy E_e and the ion energy E_i are used to calculate the relative energy of electrons and ions in the c.m. frame. A relativistic transformation yields

$$E_{\mathrm{rel}} = [A_1^2 + 2(E_i E_e + E_i m_e c^2 + E_e m_i c^2 - A_2)]^{1/2} - A_1,$$

$$A_1 = m_i c^2 + m_e c^2, \tag{7}$$

$$A_2 = [E_i E_e (E_i + 2m_i c^2)(E_e + 2m_e c^2)]^{1/2} \cos(\theta),$$

where θ is the angle between the electron- and the ion-beam directions. According to Eq. (7), the minimum relative energy $E_{\mathrm{rel}} = 0$ eV cannot be reached if an angle $\theta \neq 0$ is present. Therefore, the alignment of the beams was optimized before the recombination experiments in order to achieve $\theta = 0$ mrad with an uncertainty of 0.1 mrad.

The counting rate measured at the scanning energy E_{meas} is given by

$$R(E_{\mathrm{meas}}) = \frac{\alpha(E_{\mathrm{meas}})\,\eta L n_e(E_{\mathrm{meas}}) N_i}{C\gamma^2} + R_{\mathrm{back}} \tag{8}$$

with α denoting the electron-ion recombination rate coefficient, η the detection efficiency of the scintillator detector, which is very close to unity, $L = 2.5$ m the nominal length of the interaction zone, $n_e(E)$ the electron density at energy E, N_i the number of stored ions, $C = 108.36$ m the ring circumference, and γ the relativistic Lorentz factor for the transformation between the c.m. and the laboratory frames. R_{back} denotes the measured background rate due to collisions with residual gas molecules. In order to extract an absolute rate coefficient from the experimental data, the background has to be subtracted by taking into account the counting rate

$$R(E_{\mathrm{ref}}) = \frac{\alpha(E_{\mathrm{ref}})\,\eta L n_e(E_{\mathrm{ref}}) N_i}{C\gamma^2} + R_{\mathrm{back}}, \tag{9}$$

at a reference energy E_{ref}. Combining Eqs. (8) and (9), α at E_{meas} is calculated from

$$\alpha(E_{\mathrm{meas}}) = \frac{[R(E_{\mathrm{meas}}) - R(E_{\mathrm{ref}})]C\gamma^2}{\eta L n_e(E_{\mathrm{meas}}) N_i} + \alpha(E_{\mathrm{ref}}) \frac{n_e(E_{\mathrm{ref}})}{n_e(E_{\mathrm{meas}})}. \tag{10}$$

Because of RR, one always has a nonzero recombination-rate coefficient $\alpha(E_{\mathrm{ref}})$ at the reference point. Usually E_{ref} is chosen such that $\alpha(E_{\mathrm{ref}})$ practically equals zero, but in general one has to re-add the rate that has been neglected by subtracting $R(E_{\mathrm{ref}})$ from $R(E_{\mathrm{meas}})$ [second term in Eq. (10)]. In the present experiment, the reference rate has been measured at the maximum accessible scan energy, i.e., at $E_{\mathrm{ref}} = 125$ eV. According to RR theory, the rate coefficient at this energy is $\alpha(E_{\mathrm{ref}}) = 3.6 \times 10^{-10}\,\mathrm{cm^3\,s^{-1}}$ (see below) leading to a modification of the measured rate coefficient at $E_{\mathrm{rel}} = 0$ eV by only 0.2%.

Electron and ion beams are merged and demerged by bending the electron beam in a toroidal magnetic field with a bending radius of 120 cm. An electron beam of 2.54-cm radius is still overlapping the ion beam for 25 cm before and after the straight overlap section of 250 cm. The merging and demerging sections therefore contribute to the measured counting rate. As one can see in the left panel of Fig. 3, where the calculated potential distribution of the drift tubes for an applied voltage of 1 V is plotted against the position inside the cooler (measured from the entrance of the ion beam into the straight section of the cooler along the central axis of the ion and electron beam), the influence of the voltage applied to the drift tubes is restricted to the straight overlap section of the cooler. Thus, the electron energy in the toroidal sections is always the same independent of the drift tube potential. This results in a constant contribution to the measured counting rate, which is considered by the background subtraction procedure described above.

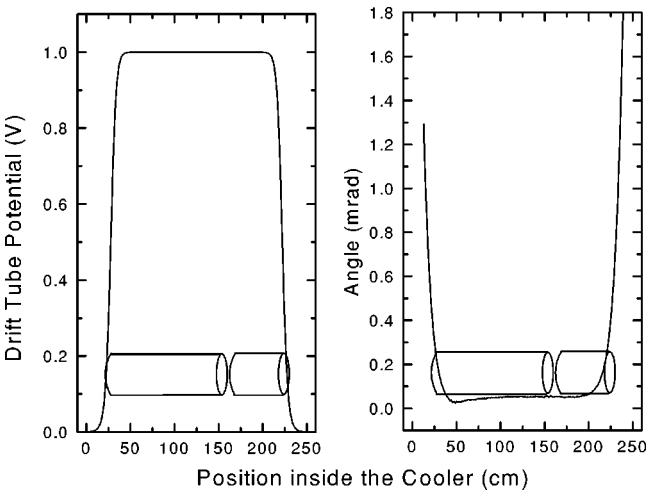

FIG. 3. Electric potential and angle θ between electron and ion trajectories along the cooler axis. The dependences are displayed along the 2.5-m-long straight section between the toroids. The position of the drift tubes covering 2 m of the interaction region is also indicated. The left panel shows the calculated electric potential along the cooler axis if a voltage of 1 V is applied to the drift tubes. In the right panel, the angle θ is shown corresponding to a measurement of the magnetic guiding field. Here, perfect alignment of the ion beam with the geometrical cooler axis is assumed, which is attainable by using the steerer magnets.

The electrons strictly follow the magnetic-field lines. Nonzero angles θ between electron trajectories and the ion-beam direction along the geometrical cooler axis result from the measured transverse magnetic guiding field components in the merging section. The *B*-field measurement was restricted to a length of 2.26 m (90% of the straight overlap section), which fully covered the drift tube region. These measured *B*-field inhomogeneities are on the 10^{-4} level. At the experimental ion energy, they give rise to motional electric fields of up to 20 V/cm. The right panel of Fig. 3 shows the resulting distribution of angles θ. As one can see, θ increases rapidly at the edges of the measured range. Both the distributions of the electric potential and angle (Fig. 3) can be combined via Eq. (7) into a distribution of relative energies along the ion-beam axis. Figure 4 shows the relative energies along the straight overlap section for different voltages applied to the drift tubes. Obviously the desired relative energies are only realized over a certain energy-dependent fraction of the whole interaction length. Consequently, the measured rate coefficient at a given relative energy E_{meas} contains contributions from other relative energies; i.e., it results from the convolution

$$\alpha(E_{\mathrm{meas}}) = \frac{1}{L}\int_0^L dl \;\; \alpha(E_{\mathrm{rel}}(l)) \tag{11}$$

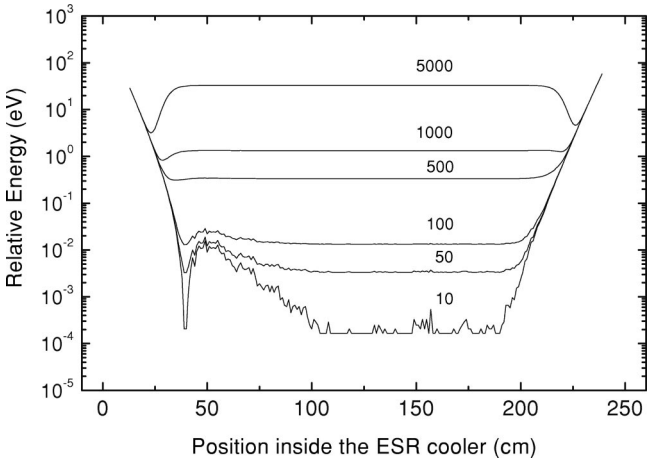

FIG. 4. Relative energies between electrons and ions along the straight overlap section inside the cooler. The energies have been calculated according to Eq. (7) taking into account the distributions of the electric potential and the angle θ (from Fig. 3). The voltages of 10, 50, 100, 500, 1000, and 5000 V applied to the drift tubes correspond to $E_{\mathrm{rel}}=1.7\times10^{-4}$, 0.003, 0.013, 0.33, 1.3, and 32.7 eV. Position 0 indicates the entrance of the ion beam into the straight section of the cooler.

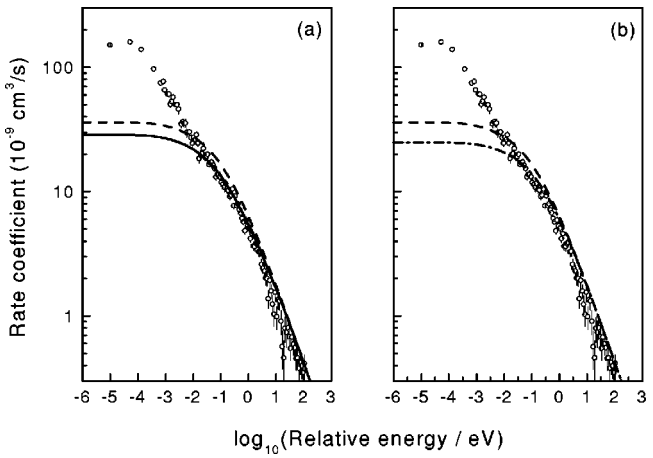

FIG. 5. Measured absolute recombination-rate coefficient of Bi^{83+} (circles) with free electrons plotted against the relative energy between electrons and ions. For the calculation of the theoretical curves in panel (a), the same electron-beam temperatures but different cutoff quantum numbers were used. In (b), the cutoff quantum number was kept fixed and the transverse temperature was changed. In detail, the parameters used were $kT_{\parallel}=0.1$ meV for all curves and $kT_{\perp}=120$ meV and $n_{\max}=n_F=116$ (full line), $kT_{\perp}=120$ meV and $n_{\max}=n_{\gamma}=442$ (dashed line), and $kT_{\perp}=250$ meV and $n_{\max}=n_{\gamma}=442$ (dash-dotted line).

with $E_{\mathrm{rel}}(l)$ being the relative energy at the position l inside the cooler. According to Eq. (11), the correct rate coefficient can be obtained by a deconvolution that is performed iteratively. In a first iteration step, the measured rate coefficient $\alpha(E_{\mathrm{meas}})=\alpha^{(0)}$ is inserted as $\alpha(E_{\mathrm{rel}}(l))$ into Eq. (11). Then the difference $\Delta\alpha^{(0)}$ between the obtained result and the measured rate is subtracted from $\alpha^{(0)}$. In a next step, the new $\alpha^{(1)}=\alpha^{(0)}-\Delta\alpha^{(0)}$ is likewise inserted into Eq. (11) and the difference $\Delta\alpha^{(1)}$ is calculated. The procedure is carried on until in a step k the relative difference $\Delta\alpha^{(k)}(E_{\mathrm{meas}})/\alpha(E_{\mathrm{meas}})$ is below 10^{-3} at all measured energies. This is the case after only a few iteration steps.

Although the relative statistical errors of the results presented below amount to less than 1% in the rate coefficient maximum, the systematic uncertainty in the absolute recombination rate coefficient has been estimated to be $\pm23\%$. This is mainly due to uncertainties in the (nondestructive) ion-current measurement and uncertainties in the deconvolution procedure described above.

For the comparison of the experimental results with RR theory, a theoretical rate coefficient α_{RR} is derived by a convolution of the theoretical RR cross section σ_{RR} [cf. Eq. (5)] with the experimental velocity distribution function $f(v_{\mathrm{rel}},\vec{v})$,

$$\alpha_{\mathrm{RR}}(v_{\mathrm{rel}})=\int \sigma_{\mathrm{RR}}(E_{\mathrm{cm}}(v))v f(v_{\mathrm{rel}},\vec{v})d^3v. \qquad (12)$$

The average longitudinal c.m. velocity v_{rel} can be calculated from $\gamma_{\mathrm{rel}}=1+E_{\mathrm{rel}}/(m_ec^2)$ with $\gamma_{\mathrm{rel}}=[1-(v_{\mathrm{rel}}/c)^2]^{-1/2}$.

In our experiment, the ion velocity distribution is negligibly narrow compared to that of the electrons due to the cooling of the ion beam to a relative momentum spread below 10^{-4} and due to the large mass difference between electrons and ions. Therefore, the distribution function $f(v_{\mathrm{rel}},\vec{v})$ is dominated by the electron velocity distribution. Considering the axial symmetry of the merged-beams experiment, two velocity coordinates are sufficient to describe the distribution: $v_{\parallel}$ the velocity component in beam direction and $v_{\perp}$ the velocity component perpendicular to the beam. The appropriate velocity (or energy) spreads are characterized by two corresponding temperatures $T_{\parallel}$ and $T_{\perp}$. Due to the acceleration of the electrons, these temperatures are quite different ($T_{\parallel}\ll T_{\perp}$) resulting in a highly anisotropic velocity distribution $f(\vec{v})$, which is therefore often called ''flattened.'' Its mathematical form is given by

$$f(v_{\mathrm{rel}},\vec{v})=\frac{m_e}{2\pi kT_{\perp}}\exp\left(-\frac{m_ev_{\perp}^2}{2kT_{\perp}}\right)\times\sqrt{\frac{m_e}{2\pi kT_{\parallel}}}\exp\left(-\frac{m_e(v_{\parallel}-v_{\mathrm{rel}})^2}{2kT_{\parallel}}\right). \qquad (13)$$

For the temperature $T_{\perp}$ characterizing the transverse motion of the electrons, one has to assume $kT_{\perp}=120$ meV, which corresponds to the cathode temperature. For the longitudinal electron motion, $kT_{\parallel}=0.1$ meV is inferred from the analysis of resonance shapes in dielectronic-recombination (DR) measurements with lithiumlike Bi^{80+} ions.

IV. EXPERIMENTAL RESULTS AND DISCUSSION

A. Comparison with theory

In Fig. 5, the measured absolute rate coefficient of Bi^{83+} with free electrons is plotted versus the relative energy from 0 eV to 125 eV. The spectrum shows the typical shape of an

RR rate coefficient with a maximum at $E_{rel}=0$ eV and a continuous decrease for increasing relative energies. For the comparison of the measured rates with RR theory, besides the temperatures $T_\parallel$ and $T_\perp$ one has to know the maximum principal quantum number n_{max} (see Sec. II). In our experiment, n_{max} is determined by field ionization in the dipole magnet that separates the parent beam and the recombined ions. A first approximation of this value is the field ionization limit n_F, which is obtained [39] from

$$n_F=\left(7.3\times 10^{10}\frac{\mathrm{V}}{\mathrm{m}}\times\frac{q^3}{F} \right)^{1/4}, \tag{14}$$

where q is the charge state of the ion and $F=v_{i,\parallel}B_\perp$ the motional electric field seen by the ions with velocity $v_{i,\parallel}$ in the transverse magnetic field $B_\perp$ of the charge-analyzing magnet. In this context, one also has to account for the possibility that high Rydberg states can decay to states below n_F, provided the ions have some time between the recombination process and the arrival at the ionizing electric field F. Therefore, a more realistic estimate for the cutoff is given by

$$n_{max}=\max(n_\gamma,n_F), \tag{15}$$

where n_γ denotes the maximum principal quantum number of Rydberg states that decay before the recombined ions arrive at the analyzing magnet and thus are saved from field ionization. A formula that provides a crude estimate of n_γ based on a number of assumptions on the population and the decay of excited states can be found in Ref. [40]. A problematic underlying assumption is that the fields seen by the ions during their flight time are considered not to change the *nl* distribution of states as it results from the initial population by radiative recombination. Changes of decay rates by Stark mixing in the fields are not accounted for but probably deserve further attention.

In the present experiment, n_F and n_γ have been calculated to be 116 and 442, respectively. A comparison of both RR rate curves resulting from Eqs. (5) and (12) is shown in Fig. 5(a). While the curve calculated with $n_{max}=n_F=116$ shows a very good agreement with the experimental data for relative energies from $E_{rel}=15$ meV to 125 eV, the curve calculated with $n_{max}=n_\gamma=442$ is somewhat higher than the experimental data especially in the energy range 0.015–1 eV. However, one can also obtain a good agreement for $n_{max}=442$ if one assumes a higher transverse electron temperature $kT_\perp=250$ meV as shown in Fig. 5(b). Since it is impossible to accurately obtain both parameters from a fit of the theoretical RR curve to the experimental spectrum for the transverse temperature, we assume $kT_\perp=120$ meV, which is in accordance with the cathode temperature. The same temperature is also suggested by accompanying DR measurements with lithiumlike Bi^{83+} ions. The choice for the transverse temperature then implies $n_{max}=n_F=116$, which we will use throughout the rest of this paper. In view of the rather crude estimations of n_{max}, this value may be justified, although it appears to be rather low. A more thorough modeling of the population and deexcitation dynamics of high Rydberg states in our experimental setup is beyond the scope of this paper and left to a future study [9]. It should be noted that the longitudinal electron temperature $T_\parallel$ has only a very little influence on the RR rate coefficient and can therefore not be inferred from a comparison with theory. This has been discussed previously by, e.g., Pajek and Schuch [23] and is just a consequence of the kinematics in electron-ion merged-beam experiments.

The shape of the experimental spectrum with an additional increase towards low energies $\leqslant 15$ meV is typical for all low-energy recombination measurements in merged-beam arrangements. At $E_{rel}=0$ eV, we obtained a maximum rate coefficient of $1.5\times 10^{-7}\,\mathrm{cm^3\,s^{-1}}$ exceeding the theoretical one of $2.9\times 10^{-8}\,\mathrm{cm^3\,s^{-1}}$ by a factor of 5.2. This rate enhancement phenomenon has already been observed at other facilities with lighter ions (see Sec. I). The present Bi^{83+} experiment provides the first quantitative determination of the rate enhancement factor ϵ for a bare ion with $Z>18$. For the light ions He^{2+}, N^{7+}, Ne^{10+}, and Si^{14+}, a $Z^{2.8}$ dependence of $\Delta\alpha=\alpha_{exp}-\alpha_{theo}$ was found in an experiment carried out at the CRYRING in Stockholm [5]. This scaling cannot be directly confirmed for Bi^{83+} where $\Delta\alpha=1.2\times 10^{-7}$ $\mathrm{cm^3/s}$ has been determined, whereas from the $Z^{2.8}$ scaling of the CRYRING data one obtains $\Delta\alpha=5.8\times 10^{-7}$ $\mathrm{cm^3/s}$, i.e., almost a factor of 5 more. However, one has to be careful with comparing results from different facilities since the experimental conditions vary drastically. Apart from the extremely high electron energy of 162 keV and the extremely high nuclear charge in the present case, the influence of the experimental parameters $kT_\perp$, $kT_\parallel$ and the magnetic guiding field B has to be considered. Previous experiments with F^{6+} and C^{6+} ions [22] have shown that the excess rate $\Delta\alpha$ scales as $(kT_\parallel)^{-1/2}$ and as $(kT_\perp)^{-1/2}$. Using the present temperatures in comparison with the Stockholm conditions, the excess rate found in the present experiment has to be multiplied by a factor of approximately $\sqrt{120\ \mathrm{meV}/10\ \mathrm{meV}}\times\sqrt{0.1\ \mathrm{meV}/0.12\ \mathrm{meV}}\approx 3.2$ in order to normalize it to the Stockholm conditions. This estimation shows that in principle the scalings could be able to essentially remove the discrepancy mentioned above. Uncertainties in the B scaling and the temperature determination prevent us from performing a more quantitative comparison.

B. Variation of the beam alignment

As mentioned already in Sec. III, the alignment of the beams has been carefully optimized before starting the recombination experiment. During the measurement, we artificially introduced an angle θ between the beams in order to check the obtained settings. This was implemented by superimposing in the interaction region a defined transverse (horizontal) magnetic field B_x in addition to the unchanged longitudinal field B_z along the ion-beam direction. Figure 6 shows the maximum recombination rate at $E_{rel}=0$ eV for different angles θ from -0.6 mrad to 0.6 mrad in the horizontal plane. At $\theta=0$ mrad, the maximum recombination rate is obtained. The open circles in Fig. 6 denote the expected rates for the selected angles. They have been determined by taking recombination rates from the ($\theta=0$ mrad) spectrum at the minimum relative energies possible at the

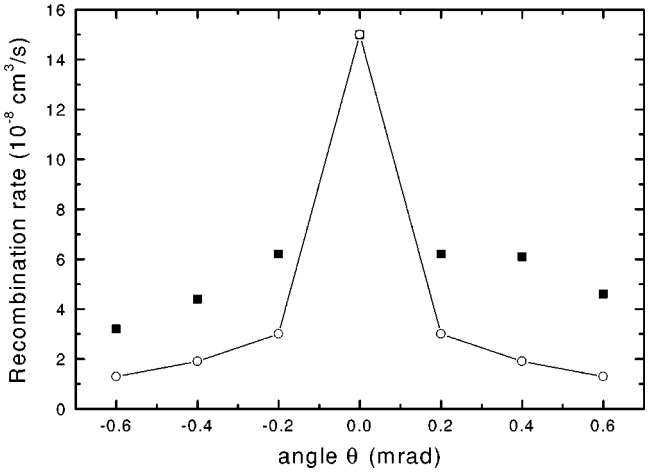

FIG. 6. Maximum recombination-rate coefficients at the lowest accessible average c.m. energy for different angles θ set between electron and ion beam. The open circles denote the values expected on the basis of the ($\theta=0$ mrad) spectrum. The measured rate coefficients are represented by the squares. The differences at angles larger than 0 mrad are most probably due to the cooling forces that steer the ion beam towards smaller angles than nominally set.

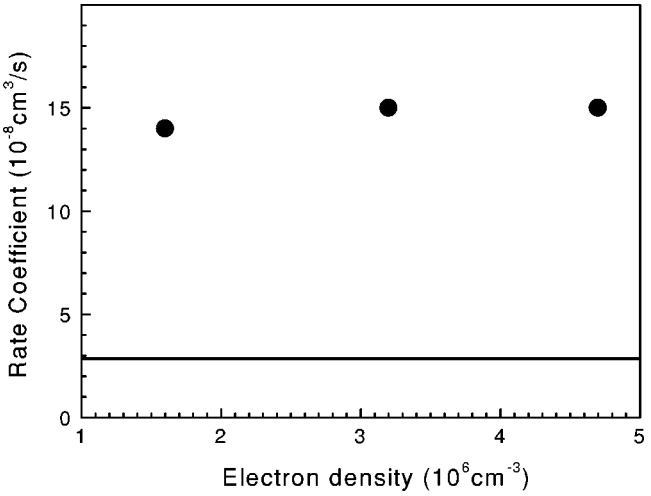

FIG. 7. Influence of the electron density on the recombination of Bi^{83+}. The full circles represent the measured rate coefficients at $E_{\mathrm{rel}}=0$ eV plotted against the electron density. The solid line shows the theoretical RR rate coefficient at $E_{\mathrm{rel}}=0$ eV calculated with $kT_{\parallel}=0.1$ meV, $kT_{\perp}=120$ meV, and $n_{\max}=116$.

corresponding angle [see Eq. (7)]. The squares in Fig. 6 represent the measured rate coefficients at the minimum relative energies E_{rel} accessible at the selected angles. All of them are lying above the expected values. Such a behavior is already known from other experiments at the ESR. Most probably it is to be attributed to the cooling forces that steer the ion beam towards smaller angles than nominally set. The important point of our observation is that the experimental rate coefficient varies symmetrically about the maximum at $\theta=0$ mrad. This confirms the accurate adjustment of the beams to within 0.1 mrad.

C. Variation of the electron density

In order to test our experimental procedure and to investigate the influence of the electron density on the recombination rate, we performed recombination measurements for three different densities $1.6\times10^6\,\mathrm{cm}^{-3}$, $3.2\times10^6\,\mathrm{cm}^{-3}$, and $4.7\times10^6\,\mathrm{cm}^{-3}$. In Fig. 7, the rate coefficient at $E_{\mathrm{rel}}=0$ eV is plotted against the electron density n_e. The solid line represents the theoretical rate coefficient calculated with $kT_{\parallel}=0.1$ meV and $kT_{\perp}=120$ meV at $E_{\mathrm{rel}}=0$ eV. There is a small difference between the maximum rate coefficient $\alpha_{\max}=1.4\times10^{-7}\,\mathrm{cm}^3\,\mathrm{s}^{-1}$ for $n_e=1.6\times10^6\,\mathrm{cm}^{-3}$ and $\alpha_{\max}=1.5\times10^{-7}\,\mathrm{cm}^3\,\mathrm{s}^{-1}$ for the two higher densities but this deviation is within the experimental uncertainty. In addition, we find that the shapes of the spectra are identical for all densities as expected for single collision conditions. Apart from a consistency check of our measurement of the RR rate coefficient, this indicates constant temperatures in the measurements with different electron densities. Therefore, it can be concluded that there is no significant influence of the electron density on the recombination rate at zero energy. This observation is in accordance with findings at the CRYRING [8], the TSR [9], and the GSI single pass electron target [10]. The lack of any density dependence of the rate at zero energy rules out TBR [Eq. (2)] as a possible mechanism leading to enhanced recombination rates at low energies. With a significant contribution of TBR to the observed rates, one would expect an increase of the recombination rate with increasing electron density in contrast to all experimental observations. In the context of storage rings, TBR has been discussed in some detail by Pajek und Schuch [17]. They found theoretically that TBR effectively populates high Rydberg states of the ion where the electrons are very weakly bound. As mentioned above, such ions are reionized in the dipole magnet and therefore do not contribute to the measured recombination rate.

D. Variation of the magnetic field

In a next stage of our experiment, we also varied the magnetic guiding field of the electron beam between 70 mT and 150 mT in steps of 1 mT. The standard field strength used for the previous measurements was 110 mT. In contrast to the more careful adjustments of the magnetic field at the TSR [22,24], which were accompanied by measurements of the cooling force and the beam profiles in order to preserve the beam quality, no other cooler setting beside the magnetic field was changed at the ESR. This procedure was motivated by an earlier experiment of the ESR cooler group with 310 MeV/u U^{92+} ions [41] that revealed a rapid oscillation of the measured recombination rate as a function of the magnetic field. The new results obtained for 295.3 MeV/u Bi^{83+} are shown in Fig. 8 (open circles), where the maximum recombination rate at $E_{\mathrm{rel}}=0$ eV is plotted versus the magnetic-field strength $B_{\parallel}$. Since the measurement of a complete recombination spectrum is very time-consuming, only the recombination rate at $E_{\mathrm{rel}}=0$ eV could be recorded for an extended range of magnetic-field settings. For these data points, a background subtraction and corrections due to the potential and angle distributions inside the cooler were not possible. Therefore, these uncorrected measured recombina-

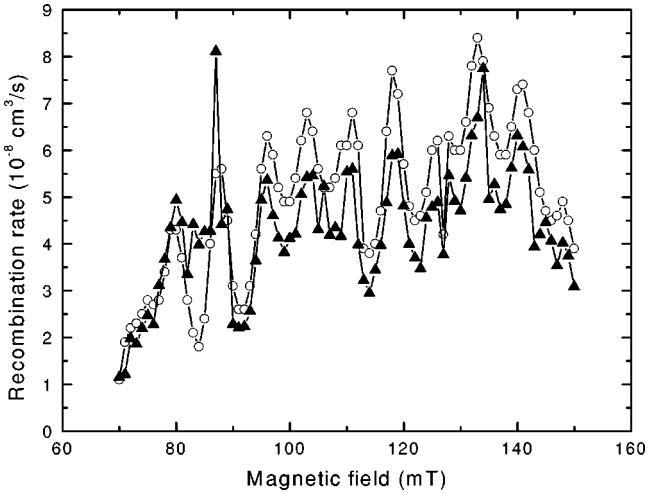

FIG. 8. Comparison of recombination-rate coefficients at $E_{\mathrm{rel}}=0$ eV obtained via two different methods. The open circles show the recombination rate calculated from the counting rate of recombined particles. These data do not include the background subtraction and corrections due to the potential and angle distribution inside the cooler. Therefore, they are lower than the rates displayed in Fig. 7. The full triangles represent rate coefficients obtained via the storage lifetime of the Bi^{83+} beam in the ring. There is a good overall agreement between the different approaches.

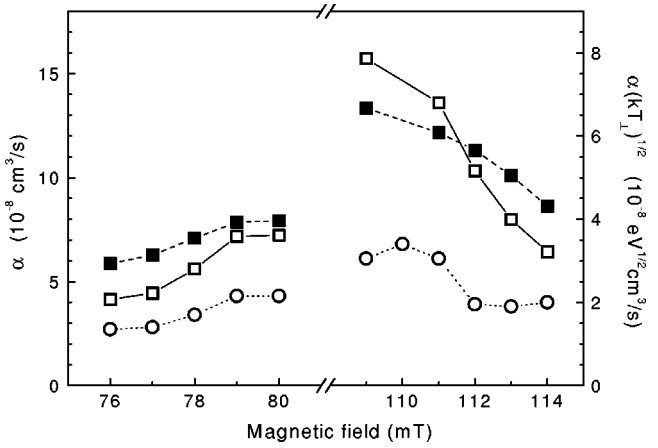

FIG. 9. Recombination rates at $E_{\mathrm{rel}}=0$ eV. The open squares (left scale) represent results from energy-dependent measurement with subsequent corrections for background and the distribution of relative energies along the axis of the cooler. The full squares (right scale) are the same results multiplied by $(kT_\perp)^{1/2}$, where $kT_\perp$ has been determined individually by comparing each energy-dependent recombination spectrum with RR theory. If the transverse temperature alone were responsible for the observed variations, the full squares would line up on a horizontal straight line. The open circles (left scale) are recombination-rate coefficients calculated from the counting rate of recombined Bi^{82+} ions taken from Fig. 8.

tion rates represented by the open circles in Fig. 8 are lower than the ones obtained from the evaluation of energy-dependent recombination measurements. Nevertheless, they qualitatively display the dependence on the magnetic field at zero relative energy. A Fourier analysis of the experimental data yields an ''oscillation period'' of the recombination rate of 7.6 mT.

A complementary method of determining the recombination rate at cooling can be applied by analyzing the lifetime of the Bi^{83+} beam in the ring. Fitting an exponential curve $I(t)=I_0\times\exp(-t/\tau)$ to the decay of the ion current stored in the ring, one can extract the storage lifetime τ of the Bi^{83+} beam in the ring. Assuming that electron-ion recombination in the cooler is the only loss mechanism for stored ions, one can calculate the corresponding recombination rate to be $\alpha_\tau=(\tau n_{\mathrm{eff}})^{-1}$ with the effective electron density $n_{\mathrm{eff}}=n_eL/C$. The full triangles in Fig. 8 represent α_τ as a function of $B_\parallel$. The good agreement between the data obtained with the two different methods underlines the consistency of our observation.

For a closer look at the oscillatory magnetic-field dependence of the recombination rate, we performed energy-dependent recombination measurements for 10 selected field strengths. We find that for $E_{\mathrm{rel}}\gtrsim 1$ eV, the measured rate coefficients are practically identical irrespective of the magnetic field. At lower energies, however, pronounced differences occur. After the application of all corrections (cf. Sec. III), the open squares in Fig. 9 are obtained as the recombination-rate coefficient at zero energy. The corrected values are higher than the ones obtained above (open circles) but exhibit qualitatively the same dependence on the magnetic field. Apart from the fact that the values derived from the energy-dependent measurements are more appropriate, a comparison of the measured recombination spectra with RR theory facilitates the extraction of electron-beam temperatures. As discussed above, the shape of the recombination spectrum is rather insensitive to even order-of-magnitude variations of the longitudinal temperature. In contrast, the transverse temperatures can be determined rather uniquely (with an estimated error of $\pm 20\%$) from the comparison between experiment and theory over the energy interval 0.1 eV$\gtrsim E_{\mathrm{rel}}\gtrsim 1$ eV, which leaves out the rate enhancement region. The transverse temperature exhibits a strong variation with the magnetic field. When, e.g., going from $B_\parallel=109$ mT to $B_\parallel=114$ mT, it changes from 170 meV to 450 meV. Across the lower magnetic-field range in Fig. 9, similar variations of $kT_\perp$ are found.

It is obvious that the recombination rate at $E_{\mathrm{rel}}=0$ and $kT_\perp$ are interrelated. In order to remove the established $(kT_\perp)^{-1/2}$ scaling of $\alpha(E_{\mathrm{rel}}=0)$, we have also plotted scaled rate coefficients $\alpha(E_{\mathrm{rel}}=0)(kT_\perp)^{1/2}$ in Fig. 9 (full squares). The scaled rate coefficients exhibit a smoother dependence on $B_\parallel$ than the unscaled ones. The ratio between the maximum (at $B_\parallel=109$ mT) and minimum (at $B_\parallel=76$ mT) scaled rate coefficient is 2.3 only, whereas for the unscaled one the ratio amounts to 3.8., i.e., part of the observed oscillations in the recombination rate at zero energy can be attributed to accompanying variations of the transverse electron temperature. It can be speculated that the remaining differences are due to undetected variations of the longitudinal temperature via the recently established [22] $(kT_\parallel)^{-1/2}$ scaling of the excess rate $\Delta\alpha$. In order to explain the remaining differences of the excess rate by variations of $kT_\parallel$, these would have to amount to a factor of ~ 8. In any case, the origin of the rather large temperature variations of already a factor of 3 for

$kT_\perp$ when applying only a 5% change to the magnetic guiding field is unclear.

It should be pointed out that the temperature dependence of the recombination rate at zero relative energy does not explain the observed general enhancement of the rate coefficient at $E_{\rm rel}=0$ eV. A further theoretical analysis should especially focus on the possible influence of the electron energy since in experiments with lithiumlike 97.2 MeV/u Bi^{80+} ions (corresponding to 53.31 kV cooling voltage instead of 162 kV for 295.3 MeV/u) during the same beam time the oscillations did not appear. This is in agreement with the results obtained at the ESR and other storage rings in experiments at low ion energies. There, oscillations of the recombination rate at cooling have never been observed. On the other hand, smooth dependences of the excess rate on the magnetic field have been reported elsewhere [10,22].

V. CONCLUSIONS

The recombination of bare Bi^{83+} ions with free electrons has been studied at the GSI Experimental Storage Ring (ESR) in Darmstadt. A critical comparison of available RR theories for Bi^{83+} has been made. Within the experimental uncertainty, the measured rate coefficient at energies from $E_{\rm rel}=15$ meV to 125 eV agrees with the semiclassical theory corrected by multiplication with energy-independent Gaunt factors. At very low c.m. energies, however, the measured rate exceeds the theoretical predictions by a factor of 5.2. Such a rate enhancement has been measured previously with lower-Z ions at other storage rings and merged-beam arrangements. Our present observation at the ESR extends the range of recombination results for bare ions to higher Z and confirms that the rate enhancement phenomenon is consistently observed in all experiments of this type.

After applying previously established scalings [22] to the measured excess rate, the present first rate enhancement result for a bare ion with Z very much greater than 18 fits roughly (with a large error bar) into a $Z^{2.8}$ dependence of the enhancement found in an experiment with the light ions He^{2+}, N^{7+}, Ne^{10+}, and Si^{14+} [5]. The increase of the electron density in the interaction area from $n_e=1.6\times10^6\,{\rm cm}^{-3}$ to $4.7\times10^6\,{\rm cm}^{-3}$ appears to have no significant effect on the recombination rate. This observation is consistent with earlier results [8–10].

A variation of the magnetic field from 70 mT to 150 mT revealed a strong dependence of the recombination rate at low energies on this parameter. The observed oscillations of the maximum recombination rate at $E_{\rm rel}=0$ eV confirmed previous observations with bare U^{92+} ions [41]. Comparing the recombination spectra with RR theory, one finds strong variations of the transverse electron temperature connected to the oscillations of the recombination rate. In future experimental and theoretical studies, this relationship has to be investigated in more detail.

The observed recombination-rate enhancement significantly reduces the lifetime of ion beams in storage rings during the electron cooling procedure. At the present ion energies, recombination in the cooler by far dominates over all factors influencing the beam lifetime. The recombination-rate enhancement hence reduces the beam lifetime by approximately a factor 5 as compared with the assumption of pure RR. Finally, we want to emphasize that it might be interesting to explore the potential of the rate enhancement phenomenon for the efficient production of neutral antimatter.

ACKNOWLEDGMENTS

The Giessen Group gratefully acknowledges support for this work through Contract GI MÜL S with the Gesellschaft für Schwerionenforschung (GSI), Darmstadt, and by a research Grant (No. 06 GI 848) from the Bundesministerium für Bildung und Forschung (BMBF), Bonn.

[1] *Recombination of Atomic Ions*, edited by W. G. Graham *et al.*, Vol. 296 of *NATO Advanced Study Institute Series B: Physics* (Plenum Press, New York, 1992).

[2] M. Holzscheiter and M. Charlton, Rep. Prog. Phys. **62**, 1 (1999).

[3] C. Wesdorp, F. Robicheaux, and L. D. Noordam, Phys. Rev. Lett. **84**, 3799 (2000).

[4] L. H. Andersen, J. Bolko, and P. Kvistgaard, Phys. Rev. Lett. **64**, 729 (1990).

[5] H. Gao, R. Schuch, W. Zong, E. Justiniano, D. R. DeWitt, H. Lebius, and W. Spies, J. Phys. B **30**, L499 (1997).

[6] A. Wolf, J. Berger, M. Bock, D. Habs, B. Hochadel, G. Kilgus, G. Neureither, U. Schramm, D. Schwalm, W. Szmola, A. Müller, M. Wagner, and R. Schuch, Z. Phys. D: At., Mol. Clusters **21**, S69 (1991).

[7] O. Uwira, A. Müller, W. Spies, A. Frank, J. Linkemann, C. Brandau, T. Cramer, C. Kozhuharov, J. Klabunde, N. Angert, P. H. Mokler, R. Becker, M. Kleinod, and N. R. Badnell, Hyperfine Interact. **108**, 167 (1997).

[8] H. Gao, S. Asp, C. Biedermann, D. R. DeWitt, R. Schuch, W. Zong, and H. Danared, Hyperfine Interact. **99**, 301 (1996).

[9] S. Schippers, A. Hoffknecht, A. Müller, G. Gwinner, D. Schwalm, and A. Wolf, Phys. Scr. (to be published).

[10] A. Hoffknecht, O. Uwira, S. Schennach, A. Frank, J. Haselbauer, W. Spies, N. Angert, P. H. Mokler, R. Becker, M. Kleinod, S. Schippers, and A. Müller, J. Phys. B **31**, 2415 (1998).

[11] A. Müller, S. Schennach, M. Wagner, J. Haselbauer, O. Uwira, W. Spies, E. Jennewein, R. Becker, M. Kleinod, U. Pröbstel, N. Angert, J. Klabunde, P. H. Mokler, P. Spädtke, and B. Wolf, Phys. Scr. **T37**, 62 (1991).

[12] D. M. Mitnik, M. S. Pindzola, F. Robicheaux, N. R. Badnell, O. Uwira, A. Müller, A. Frank, J. Linkemann, W. Spies, N. Angert, P. H. Mokler, R. Becker, M. Kleinod, S. Ricz, and L. Empacher, Phys. Rev. A **57**, 4365 (1998).

[13] O. Uwira, A. Müller, J. Linkemann, T. Bartsch, C. Brandau, M. Schmitt, A. Wolf, D. Schwalm, R. Schuch, W. Zong, H.

Lebius, W. G. Graham, J. Doerfert, and D. W. Savin, Hyperfine Interact. **108**, 149 (1997).
[14] S. Baird, J. Bosser, C. Carli, M. Chanel, P. Levèvre, R. Ley, R. Maccaferri, S. Maury, I. Meshkov, D. Möhl, G. Molinari, F. Motsch, H. Mulder, G. Tranquille, and F. Varenne, Phys. Lett. B **361**, 184 (1995).
[15] G. F. Gribakin, A. A. Gribakina, and V. V. Flambaum, Aust. J. Phys. **52**, 443 (1999).
[16] L. Bureyeva and V. Lisitsa, J. Phys. B **31**, 1477 (1998).
[17] M. Pajek and R. Schuch, Hyperfine Interact. **108**, 185 (1997).
[18] Y. Hahn and P. Krstić, J. Phys. B **27**, L509 (1994).
[19] Y. Hahn and J. Li, Z. Phys. D: At., Mol. Clusters **36**, 85 (1996).
[20] G. Zwicknagel, C. Toepffer, and P. G. Reinhard, Laser Part. Beams **13**, 311 (1995); Hyperfine Interact. **99**, 285 (1996).
[21] Q. Spreiter and C. Toepffer, Hyperfine Interact. **114**, 245 (1998); J. Phys. B **33**, 2347 (2000).
[22] G. Gwinner, A. Hoffknecht, T. Bartsch, M. Beutelspacher, N. Eklöw, P. Glans, M. Grieser, E. Lindroth, A. Müller, A. A. Saghiri, S. Schippers, D. Schwalm, G. Wissler, and A. Wolf, Phys. Rev. Lett. **84**, 4822 (2000).
[23] M. Pajek and R. Schuch, Phys. Rev. A **45**, 7894 (1992).
[24] A. Hoffknecht, T. Bartsch, S. Schippers, A. Müller, N. Eklöw, P. Glans, M. Beutelspacher, M. Grieser, G. Gwinner, A. A. Saghiri, and A. Wolf, Phys. Scr. **T80**, 298 (1999).
[25] T. Stöhlker, P. H. Mokler, C. Kozhuharov, and A. Warczak, Comments At. Mol. Phys. **33**, 271 (1997).
[26] T. Stöhlker, T. Ludziejewski, F. Bosch, R. W. Dunford, C. Kozhuharov, P. H. Mokler, H. F. Beyer, O. Brinzanescu, B. Franzke, J. Eichler, A. Griegal, S. Hagmann, A. Ichihara, A. Krämer, J. Lekki, D. Liesen, F. Nolden, H. Reich, P. Rymuza, Z. Stachura, M. Steck, P. Swiat, and A. Warczak, Phys. Rev. Lett. **82**, 3232 (1999).
[27] H. A. Kramers, Philos. Mag. **46**, 836 (1923).
[28] M. Stobbe, Ann. Phys. (Leipzig) **7**, 661 (1930).
[29] H. A. Bethe and E. E. Salpeter, *Quantum Mechanics of One- and Two-Electron Systems* (Springer, Berlin, 1957).
[30] K. Omidvar and P. T. Guimaraes, Astrophys. J., Suppl. **73**, 555 (1990).
[31] M. R. Flannery, in *Atomic, Molecular & Optical Physics Handbook* (AIP, New York, 1996), p. 625.
[32] E. Zerrad and Y. Hahn, J. Quant. Spectrosc. Radiat. Transf. **59**, 637 (1998).
[33] L. H. Andersen and J. Bolko, Phys. Rev. A **42**, 1184 (1990).
[34] A. Ichihara and J. Eichler, At. Data Nucl. Data Tables **74**, 1 (2000).
[35] T. Stöhlker, C. Kozhuharov, P. H. Mokler, A. Warczak, F. Bosch, H. Geissel, R. Moshammer, C. Scheidenberger, J. Eichler, A. Ichihara, T. Shirai, Z. Stachura, and P. Rymuza, Phys. Rev. A **51**, 2098 (1995).
[36] V. M. Shabaev, Y. A. Yerokhin, T. Beier, and J. Eichler, Phys. Rev. A **61**, 052112 (2000).
[37] B. Franzke, Nucl. Instrum. Methods Phys. Res. B **24/25**, 18 (1987).
[38] H. Horneff, Patentschrift DE 4040164 C2 (Deutsches Patentamt, 1992).
[39] A. Müller, D. S. Belić, B. D. DePaola, N. Djurić, G. H. Dunn, D. W. Mueller, and C. Timmer, Phys. Rev. A **36**, 599 (1987).
[40] A. Müller, and A. Wolf, Hyperfine Interact. **107**, 233 (1997).
[41] M. Steck (unpublished).